SSRG International Journal of Electrical and Electronics Engineering
ISSN: 2348-8379/ https://doi.org/10.14445/23488379/IJEEE-V10I7P107

Volume 10 Issue 7, 76-92, July 2023

Original Article

An Adaptive Segmentation Approach with IWT-AWT Modeling with Hybrid Ensemble Algorithm for Skin Cancer Classification

Ravi Chandra Bandi[1], K. Rajendra Prasad[2], A. Kamalakumari[3], A. Daisy Rani[4]

[1,3,4]*Department of Instrument Technology, Andhra University College of Engineering, Visakhapatnam, India.*
[2]*Department of Computer Science & Systems Engineering, GITAM University, Visakhapatnam, India.*

[4]*Corresponding Author : dr.adaisyrani@andhrauniversity.edu.in*

Received: 29 April 2023 Revised: 27 June 2023 Accepted: 18 July 2023 Published: 31 July 2023

Abstract *- With the common occurrence of the different types of cancers, skin cancer is a frequently observed characteristic problem rooted in significant body parts. Many problems related to identifying the different types of cancer are to be analyzed that are not visible, or the type is quite complicated to identify the root of the problem and its occurrence. Deep learning methods and other machine learning models have been developed to introduce the overall design perspective indicating the practical approach to identification and diagnostics. Due to substantial changes in human characteristic traits/behaviour, the need of importance on lesion detection is enactive to implicate the correct problem. One such feature with region identification and transformative approach is improvised to diagnose the area and regions of cancers as effectively as possible. Our proposed approaches with IWT-AWT (Improved Watershed Transform - Active Wavelet Transform) have implicated the region structural changes via probabilistic technique to identify the correct and nearest region of the growth, indicating the overall feature traits to indicate the identification of the cancerous region. This approach (IWT-AWT) for which skin cancer on this perspective was to analyze the problem of early detection via segmentation. The overall expected conditionality approaches on the IWT-AWT algorithms have been inculcated to realize the 450 training and testing images with melanoma, Nevus, and other lesion identifications in MATLAB; we have observed the different classification accuracies, precision, and other performance metrics (Sensitivity and Specificity) are considered for the machine learning algorithms having the overall accuracies for most of the design algorithm based on IWT-AWT is 99%. On a different comparative scale, we have introduced CNN, which provides classification accuracy at 90%.*

Keywords *- AWT (Active Wavelet Transform), CNN (Convolutional Neural Networks), EC (Expected Conditionality), IWT (Improved Watershed Transform), KNN (K – Nearest Neighbours), SVM (Support Vector Machine).*

1. Introduction

Several subtypes of cancer may affect humans. However, cancer of the skin is by far the most prevalent variety [1]. It significantly impacts the number of people with lighter skin in Europe, North America, and Australia. There are two primary categories of skin cancer, which are referred to as non-melanoma and melanoma (basal cell, squamous cell, and Markel cell carcinomas, etc.). Melanoma is a more severe kind of cancer that, if not treated, may be deadly. Melanoma has a great chance of being cured if caught in its early stages, but it is incurable if it has progressed to a later stage. Malignant melanoma is the kind of skin cancer that reports the highest number of deaths and is growing at an alarming rate throughout the globe. It is also the most hazardous of the skin cancer types. More than 5,500 people in Canada have been diagnosed with melanoma, and around 17.35 percent died in 2010. Melanoma affected approximately 22,000 people in the United States in 2012, with approximately 49.4 percent dying due to the disease. In today's world, artificial intelligence encourages the rapid development of technology to detect skin cancer.

The federated skin cancer detection model (FSDM) and the dual generative adversarial network model (DGANM) are two models that help solve the problems of data fragmentation and privacy to a certain extent. According to the Cancer Trends Progress Report published by the National Institutes of Health of the United States (NIH) [4], it is anticipated that about half of all Americans who survive to the age of 65 will be diagnosed with skin cancer at some point during their lifetime [5].

The most potent weapon against this kind of cancer is discovery at an earlier stage. The so-called ABCD rule is the primary criterion used to separate benign skin lesions from malignant skin lesions. So that a diagnosis can be made, this criterion looks at the skin lesions' asymmetry, edge, colour, and size [6].

Dermoscopy is a non-invasive method of examining the skin that allows for the acquisition of an image of the skin cancer lesions that have been enlarged and lighted [7]. Dermoscopy imaging techniques improve the visual effects of the regions of interest to obtain very detailed and deeper levels of skin lesion regions by removing the surface reflection of the skin lesion [8].

Fundamentally, sizeable intra-class variances can be observed in colour, textures, shape, size, contrast, and position. Additionally, there is a very high degree of analogy between melanoma and non-melanoma lesions, which makes this problem even harder. Secondly, at the very early stage of this cancer, the automatic skin lesion recognition task becomes more complex due to low contrast and obscuration between the affected areas on the skin and standard skin regions. Thirdly, several artefacts, including hairs, veins, ruler marks, and colour calibration, may blur and occlude the skin cancer lesions, thus further reducing the recognition performance.

1.1. Problem Statement Contributions

- Implement the IWT-AWT transform model by segmenting the lesion.
- Implicate the type of cancer with input characteristic entropy with the EC model.
- Classify the cancer images with CNN, KNN, SVM, Ensemble-Bag and Stacked classifier.

2. Related Work

The categorization was carried out with the assistance of the Convolutional Neural Network (CNN) algorithm in [1] when we were working with the deep learning approach. The data are separated into benign cancer sets and cancer sets that are malignant according to this categorization.

In the end, the data offered by the logistic regression technique were analyzed, and success charts of each kind were generated and compared. As a direct consequence, accuracy and loss charts for the two kinds of cancer were generated. Utilizing the deep learning approach, the purpose of the research is to make a comparison between breast cancer and skin cancer. In addition, there is a tendency for doctors to mix breast cancer with skin cancer diagnosis. In further research, the findings of this study will serve as the foundation for distinguishing the diagnosis of these two distinct forms of cancer from one another. Our skin cancer identification model was trained on the International Skin Imaging Collaboration's Skin Cancer MNIST dataset using a MobileNetV2 for recognition and a U-Net for border segmentation. We then installed both models onto a Raspberry Pi and turned it into a helpful gadget that takes a close-up image and swiftly rescreens the patient's skin. This study showed that a Raspberry Pi could handle intensive computing like deep learning and be bundled into a cheap portable device for screening.

This research in [2] proposes utilizing deep learning to classify skin cancer efficiently. We tweaked the pre-trained Mobile Net convolutional neural network model and trained it on the HAM1000 skin lesion dataset. This transfer learning approach's weighted average of precision, Recall, and categorization accuracy is 0.97, 0.90, and 0.91, respectively. It is quick, light, and trustworthy. Medical dermatologists should diagnose skin cancer immediately. This research examines how CLAHE and MSRCR contrast improvements with CNN affect image processing. CLAHE outperforms MSRCR in CNN-based colour picture enhancement for skin cancer diagnosis. In training and validation, the original and CLAHE-enhanced datasets are equally accurate.

This research showed that skin cancer screening does not need picture contrast augmentation. Also, with three CNN models on a nine-class skin cancer classification job and integrates the most accurate model into a web application. VGG-16, VGG-19 and a self-designed CNN are compared. Since the three models differ in depth, the relationship between depth and performance within the dataset was also examined. The most accurate model, VGG-19, has 0.9290 accuracy and 1.2842 loss, making it a viable skin cancer detection aid. This article proposes an intelligent skin cancer screening method. Skin cancer is one of the worst illnesses. Thus, a fully automatic deep learning system can detect it early and save lives.

This study in [3] classifies skin cancer images using the HAM10000 dataset. Deep-SkinNet is evaluated for skin cancer categorization. Comparing Deep-SkinNet against Alex-Net, VGG-16, and InceptionV3 for skin lesion categorization All models are trained on the same dataset to derive their confusion matrices. Accuracy, precision, and Recall are assessed. Finally, the proposed model outperforms other models in experimental studies. DeepSkin-Net has 97.354% accuracy, 98% precision, 97% recall, and a 97% F1 score. Asymmetry, border irregularity, compact index, fractal dimension, edge abruptness, colour variation, and diameter are common skin cancer image analysis characteristics.

Image segmentation helps automated skin cancer detection systems identify and analyze such characteristics. This work proposes SVM-based picture segmentation using Snake active contour. SVM helps discover snake algorithm parameters. An intelligent system classifies skin cancer photos reliably to save time and effort. Intelligent machines identify skin cancer photographs by kind using a deep learning (CNN) algorithm. Basal cell carcinoma (BBC),

melanocyte nevus (NV), and vascular lesion (VASC) are employed in this investigation. The study found that using deep learning to classify and recognize skin cancer images by type may be the best way to improve early diagnosis and diagnosis accuracy. This effort yielded 98.89% accurate results.

Today, skin cancer is a leading cause of death. Exposure to sunlight may induce carcinoma, an abnormal skin cell development. Early detection cures most skin cancers. Early detection saves lives. A biopsy diagnoses carcinoma. A biopsy removes somatic cells for lab testing. It is laborious. Autonomous software-aided systems are needed for precise and rapid processing. Quantitative factors will improve target comprehension. This method in [5] detects carcinoma using SVM classifiers and malignant area characteristics. Dermoscopy images are pre-processed to remove noise, strengthen the standard, and then segmented using thresholding. The classifier receives picture characteristics via the GLCM approach. The classifier classifies images as malignant or noncancerous. This method's 94.05% accuracy beats the current systems.

In the USA, skin cancer is the most frequent. Skin cancer affects all races, genders, and ages. Melanoma lesions have an irregular form, size, and rough edge and cannot be cut in half. It also kills the most people globally. Over 5 million Americans are diagnosed annually. Melanoma is the deadliest skin cancer. Skilled physicians have manually seen and diagnosed melanoma, which is Error-prone and time-consuming. Dermoscopy photos show deeper skin layers without surface reflection. Despite this, skin lesion images include various artefacts, sounds, and complicated structures. These complicated pictures make boundary detection, feature extraction, and classification complex.

Better image classification techniques are needed to detect and forecast early melanoma. Thus, early melanoma detection, classification, and prediction require efficient, effective, and accurate methods. This poster reviews and analyses CNN and RNN classification deep learning algorithms on skin lesion images. It tests them with publicly available International Skin Imaging Collaboration (ISIC) archive large data sets. Pre-processing and resizing ISIC raw datasets will make them algorithm-friendly. Five parameters, including ROC, will be used to evaluate these methods.

Melanoma is the deadliest skin cancer. Melanoma kills many skin cancer patients. Melanocytes, which generate melanin, produce it. Before cancer spreads, detect and treat cancerous changes. Dermatologists use dermoscopy to see skin patches in melanoma patients better. Dermatologists work hard and take their time. Dermatologist screening and biopsy for severe melanoma detection Dermoscopy is slow and incorrect. The EfficientNetB6 algorithm provided a deep-learning solution. EfficientNEtB6 is used because Efficient Net models outperformed other CNNs at ImageNet in accuracy and productivity. This research proposes deep learning for non-invasive computer vision-aided medical clinical diagnosis. The suggested method employs the Efficient-NetB6 algorithm trained fivefold on a dataset of thirty thousand skin lesion pictures to identify melanoma early by estimating its likelihood.

Worldwide, skin cancer is common. Untreated malignant skin tumours may kill. SCC, MEL, and BCC are invariably cancerous and may kill the skin. Early detection reduces damage. Transfer learning and fine-tuning of the renowned pre-trained model XCEPTION helped diagnose eight skin tumours in this research. Data augmentation approaches provide a variety of model training. The ISIC 2019 dataset is used to test the approach. It can identify malignant skin tumours earlier than comparable investigations.

Since many people died from skin cancer recently, classifying them with a small dataset would be more challenging. This article in [4,6] tested models with and without pre-training to improve skin cancer binary classification accuracy. Three prominent models—Inception3, Xception, VGG16, MobileNet, and ResNet—were suggested. This research also tests popular ImageNet pre-trained models on this task. Popular approaches consecutively link the dropout, global average pooled, and output layers to meet the result condition. Several models have been evaluated by controlling variables with different hyperparameter settings like epochs, batch size, and image size. According to studies, simpler hypotheses converged faster on this restricted dataset than complicated models. Pre-training does not affect model resolution and enhances the efficiency of trained models on this dataset.

Skin cancer is the most frequent malignancy in the US and globally, according to the Skin Cancer Foundation. Early skin cancer detection and treatment may improve survival rates. Dermatologists must visually analyze dermoscopic pictures, which is time-consuming and error-prone. Automated skin lesion segmentation and categorization using deep learning have improved skin cancer detection and therapy. This study in [7] builds a mask R-CNN model for lesion segmentation utilizing pre-trained weights from the Microsoft COCO dataset after image processing. To train a mask R-CNN model for skin lesion classification, the weights of the trained model are preserved and transferred.

Our trials employ the same metrics as the International Skin Imaging Collaboration 2018 (ISIC 2018) benchmark datasets. Lesion border segmentation and categorization had 96% and 80% adjusted multiple-class accuracy, respectively. Employing the Convolutional Neural Network (CNN) technique to classify skin cancer uniquely and evaluate the SVM strategy, this study used CNN and SVM algorithms to

diagnose skin cancer and assess its accuracy. Two distinct sets are quantitatively analyzed with 20 samples and 80% pre-test quality. CNN has 95.03% accuracy, and SVM has 93.04%. The average, standard deviation, standard error, and independent sample test (if the significance is less than one) will be used to calculate the sample size. Statistics show that the algorithm's accuracy (0.490), specificity (0.009), and p > 0.05 significant values are all p 0.05. CNN outperformed SVM [8] for skin cancer detection.

Malignant cetaceous tumours have a high mortality and morbidity rate. A skin cancer diagnosis is essential since early detection may cure it. In recent years, deep learning and image processing [9]-[15] have enabled several skin cancer classification algorithms. Public techniques are used less. This research in [9] develops a convolutional neural network (CNN)-based online application to accurately identify skin cancer.

First, the Dull Razor algorithm removes skin hairs from the HAM10000 [16-20] dataset to reduce distraction. Random oversampling and data augmentation are employed to expand the dataset for overfitting. Four maximum pooling layers minimize noise, while eight convolutional layers extract features. Batch normalization and dropout layers can reduce overfitting and accelerate training. Then the Nadam optimizer compiles the model with a 0.002 learning rate and 128 batch sizes for 100 epochs. The CNN model achieves 0.9703 accuracy and 0.0844 losses on testing data. The algorithm uses Flask to anticipate skin photos from users.

In this technological age, intelligent computers using various algorithms must solve the global skin cancer problem. An intelligent system classifies skin cancer photos reliably to save time and effort. Intelligent machines identify skin cancer photographs by kind using a deep learning (CNN) algorithm [21, 22]. Basal cell carcinoma (BBC), melanocyte nevus (NV), and vascular lesion (VASC) are employed in this investigation. The study found that using deep learning to classify and recognize skin cancer images by type may be the best way to improve early diagnosis and diagnosis accuracy.

This effort yielded 98.89% accurate results. Lack of data, particularly annotated data for supervised learning algorithms, is one of the critical reasons deep learning systems for cancer diagnosis are delayed. This study introduces a CNN for skin cancer detection. The International Skin Imaging Collaboration (ISIC) provides the core database of 97 members (50 normal and 47 malignant) to train the CNN algorithm. A generative adversarial network (GAN) generates synthetic skin cancer pictures to train the CNN algorithm without data. The trained CNN's classification performance is approximately 53% without synthetic pictures, but adding them to the core database boosts it to 71% [23].

Cancer is a global killer. One in three malignancies worldwide is skin cancer. Some estimates say one in five Americans will develop skin cancer. Skin cancer therapy relies on early diagnosis. Malignant and benign skin lesions seem identical, making it difficult to differentiate them without a clinical instrument. One study found that approximately 5,000 children are biopsied each year to identify 400 melanomas, resulting in needless biopsies. We created an upgraded image classification algorithm to help dermatologists diagnose without a costly biopsy. This [24, 25] model can distinguish seven skin lesions. HAM10000 was analyzed. We classified using transfer learning with several pre-trained models, class-weighted loss, and data augmentation. Experimental results reveal that the updated ResNet50 model can classify skin lesion pictures into one of seven groups with 90 percent categorical accuracy, 0.89 weighted averages precision and 0.90 recalls. Dermatologists may use our model as a diagnostic-aid.

Skin cancer is infectious and spreads quickly. Dermatologists find it challenging to distinguish between skin cancer and rashes. People and physicians call skin changes like infections, allergies, and illnesses rashes. Knowing the differences between rashes and skin cancer can help a person seek help or avoid anxiety about a noncancerous rash. Dermatologists identify skin cancer from rashes when the skin does not heal after medication and spreads rapidly to other parts of the skin. The material helps identify skin cancer by distinguishing it from rashes. Previous studies used image classification to categorize skin cancer types. This method uses CNN [convolutional neural network] to detect and classify skin cancer and rash photos. The algorithm classifies images as skin cancer or rashes with 80.2% accuracy after 20 epochs.

A deep learning-based skin cancer diagnostic method programmatically detects melanoma cancer in dermoscopic pictures. Unrepaired deoxyribonucleic acid (DNA) causes mutations. Mutations accelerate skin cell growth, causing malignant tumours. This technique quickly and accurately detects early-stage melanoma skin cancer. Our methodology addresses the high costs, low identification accuracy, and manual detection system portability issues. Our multi-layered CNN model classifies dermoscopic pictures to diagnose skin cancer. Our model has 95.24% accuracy, 1.6% higher than the previous model. Cell proliferation damages tissues in cancer. Studies are needed to enable professionals to diagnose skin cancer, a prevalent kind of cancer, without technology support. A deep learning model with seven convolution layers and three neural layers was used to categorize the HAM10000 dataset, which comprises dermoscopic pictures, into seven groups. The model's test data accuracy was 99.01%. This suggests that the suggested methodology may assist specialists in diagnosing skin cancer [27].

Table 1. Representing the tabulated version of the literature survey

S. No	Ref. No	Authors	Algorithms	Year	Research Gap
1	2	Chee Jen Ngeh et al.	U-NET, CNN	2022	LSTM, TNN and other SOA architectures are not compared for better accurate models.
2	7	Prachya Bumrungkun et al.	SVM, decision trees, logistic regression, and snake model	2022	No deep learning models with hybrid logic are not discussed.
3	11	Jignyasa Sanghavi et al.	Backpropagation Net	2021	No User Interface prediction models with Real-time datasets have not been implemented.
4	19	Lin Li et.al	CNN	2022	Specific Weight Features on other loss characteristics, such as cross entropies, were not discussed.
5	24	Pooyan Sedigh. et al.	Deep convolutional neural networks/GAN Improvised	2022	Only Genetic Images were considered; new images on Real-time datasets with hospital records have not been utilized for real-time prediction.
6	9	Usharani Bhimavarapu et al.	Fuzzy GC-SCNN	2022	99.75% accuracy/ precision is observed. NIL.

From the above Table-1, we have demonstrated the research gaps that have been recent trends in the design of skin cancer detection for implicating the deep learning architectures. So, to provide such changes, we have also considered the designs of skin cancer detection with techniques ABCD, U-NET and CNN for realizing the overall design perspective. These changes on the cancerous images are effective in different performance metrics indicated in tabulations when compared with proposed design algorithms. The section-3 introduces such features of techniques utilized for implementing skin cancer detection.

3. Different Approaches for Lesion Detection

3.1. The ABCD Rule

The author in [11] developed the ABCD criteria for dermatologists to utilize in identifying pigmented lesions to estimate the risk of malignancy. In addition to its computation speed, this method may give a more objective and repeatable diagnosis of skin malignancies. Based on four factors, it is called one side of a mole or birthmark does not match the other.

A stand for ASYMMETRY: It is divided into two halves by orthogonal axes; each of the two axes is evaluated for any form, colour, or dermoscopic structural asymmetries. If there is asymmetry on both axes, the score is two; if there is only one axis of asymmetry, the score is one; otherwise, the score is zero.

B for ‘BORDER’ means ‘irregular, ragged, notched, or blurred’ in this context.

The letter (C) stands for Hue: The colour is not uniformly brown or black but may contain red, white, or blue flecks. We are looking for the six primary hues (white, red, light brown, dark brown, blue-grey, and black). Each preexisting colour adds one point to the score.

The term D is as Dimensions greater than 6 millimetres (approximately 1/16 of an inch or the size of a pencil eraser). The following formula is used to arrive at the result (Total Dermoscopy Score – TDS): In order to calculate the TDS, enter [(A score 1.3) + [B score 0.1] + [C score 0.5%] + [D score 0.5%] into the formula. The diagnosis is derived from Table 1 once the TDS has been computed.

Table 2. Total dermoscopic score

Total Dermoscopic Score (TDS)	Interpretation
< 4.75	Benign Melanocytic Lesion
4.8 – 5.45	Suspicious Lesion
>5.45	Lesion Highly Suspicious Melanoma

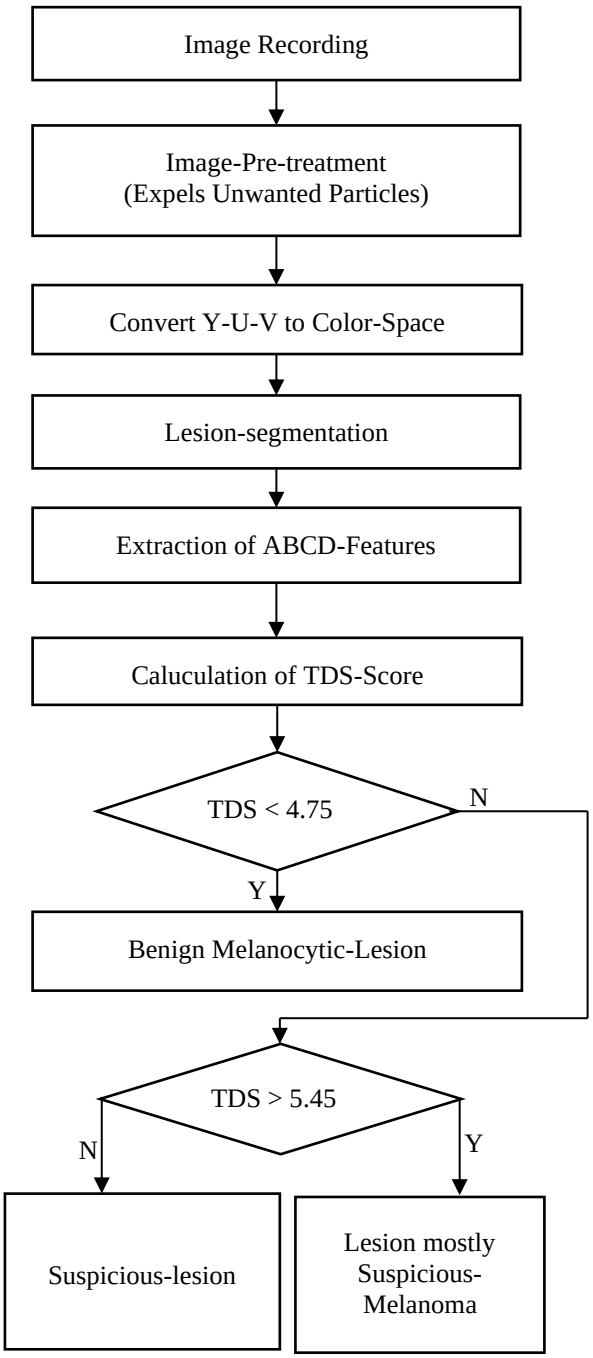

Fig. 1 The overall Flow diagram for the ABCD model

3.2. Machine/Deep Learning Approach

The system is first trained using a training dataset for systematically detecting cancer stages in melanoma and then tested. A training dataset is a trained data file for learning. A test dataset follows the same likelihood function as the training dataset, but it is independent of the training dataset. Next, the data were classified using the CNN classification method to determine the patient's stage of melanoma. CNN is employed for classifying because the database has many records, which requires much time to classify.

3.3. Other Methods

The NABLA N network (N-Net) is a novel framework for identifying skin cancer. Here, we can see the model in action in Figure 2. This newly suggested N-Net model drastically differs from the current Nabla-Net [17].

Although Nabla-Net uses FCN, N-Net relies on the R2U network paradigm. Though Nabla-Net uses only one latent space, the suggested N-Net employs many implicit spaces that effectively regenerate the learnt features. As a direct result of the Dense-Net model [23], this idea dramatically aids in reducing the number of network parameters.

Regarding attributes, in this manner, the Nabla-Net combines the second layer of the encoding unit's feature set with the 14th layer of the decoding unit's feature set. On the other hand, the N-Net uses a fusion of information from the encoding and decoding units and the decoded units themselves differently. When compared to Ladder-Net and Fusion-Net, however, as a result, the number of network parameters is greatly expanded in these numerous U-Net models. However, the encoding unit's learned latent areas are reused in the N-Net model, reducing connection weights.

These methods effectively improvise the different conditions, features and other filtering aspects on the images to identify the correct predicted cases; the overall design performance of the models is indicated in table-3. The accuracy, sensitivity and specificity are considered to realize the best-performed algorithm.

4. Proposed Algorithm with IWT-AWT

In section III, ABCD rules, deep learning approaches with CNN, dense and U-Net are implemented to analyze the regions and their texture model. Our design with IWT-AWT would suffice the correct regions weighing from different thresholds to effectively analyze the boundaries and their classification features and solve the design characteristic problems mentioned in section-1.

From this perspective, our design can analyze the different colours and texture shapes via the proposed hybrid segmented approach with a variable threshold. The possible changes in similarities of melanoma and other non-melanoma lesions are effectively classified with the type of Expected conditional Entropies, which would vary for each type of cancer's image.

The region identification with proposed IWT and AWT are utilized to identify the segmented region encapsulating the different features of the images chosen. Finally, a Kaggle dataset is utilized with different lesion changes and its region on the skin, specifically the face and neck, are demonstrated with KNN, ENSEMBLE with BG and Stacked Classification with other machine learning algorithms via IWT and AWT, which improves the classification accuracy and reaches 99%.

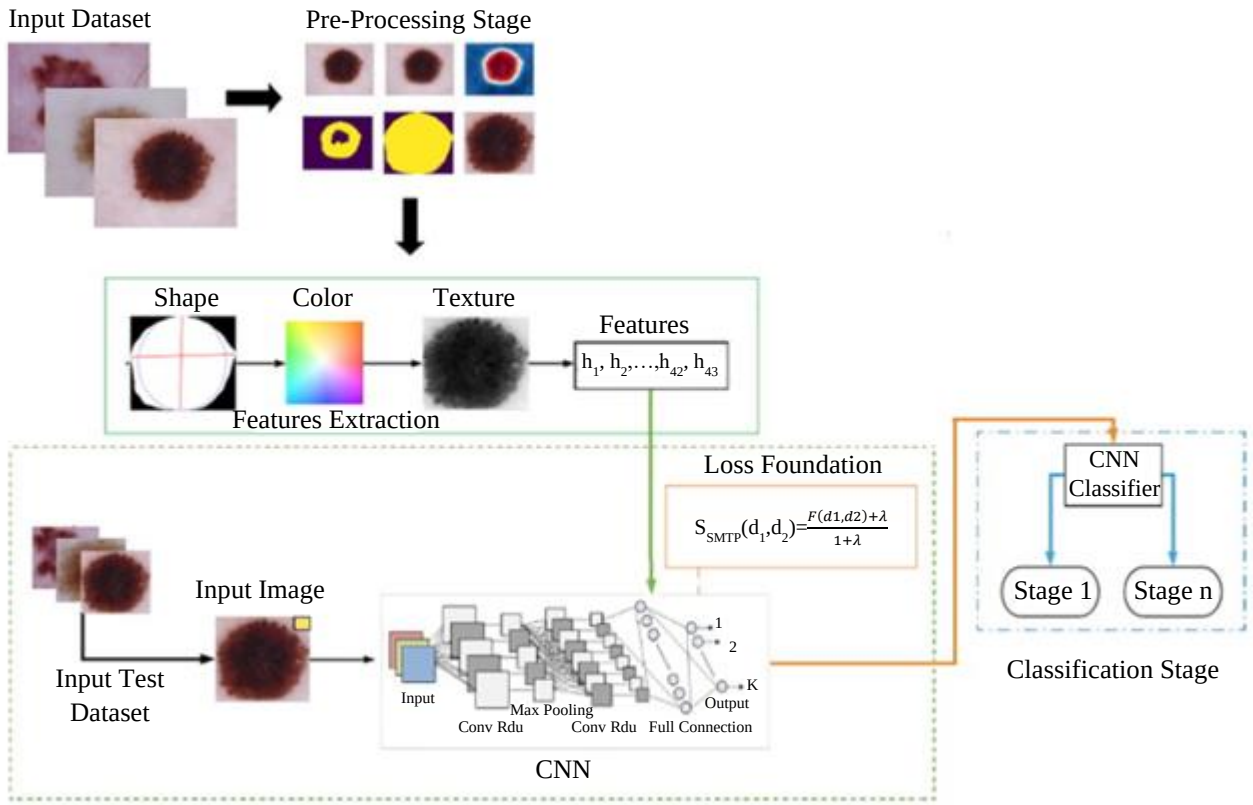

Fig. 2 The deep learning with CNN and loss function feature for stage classification

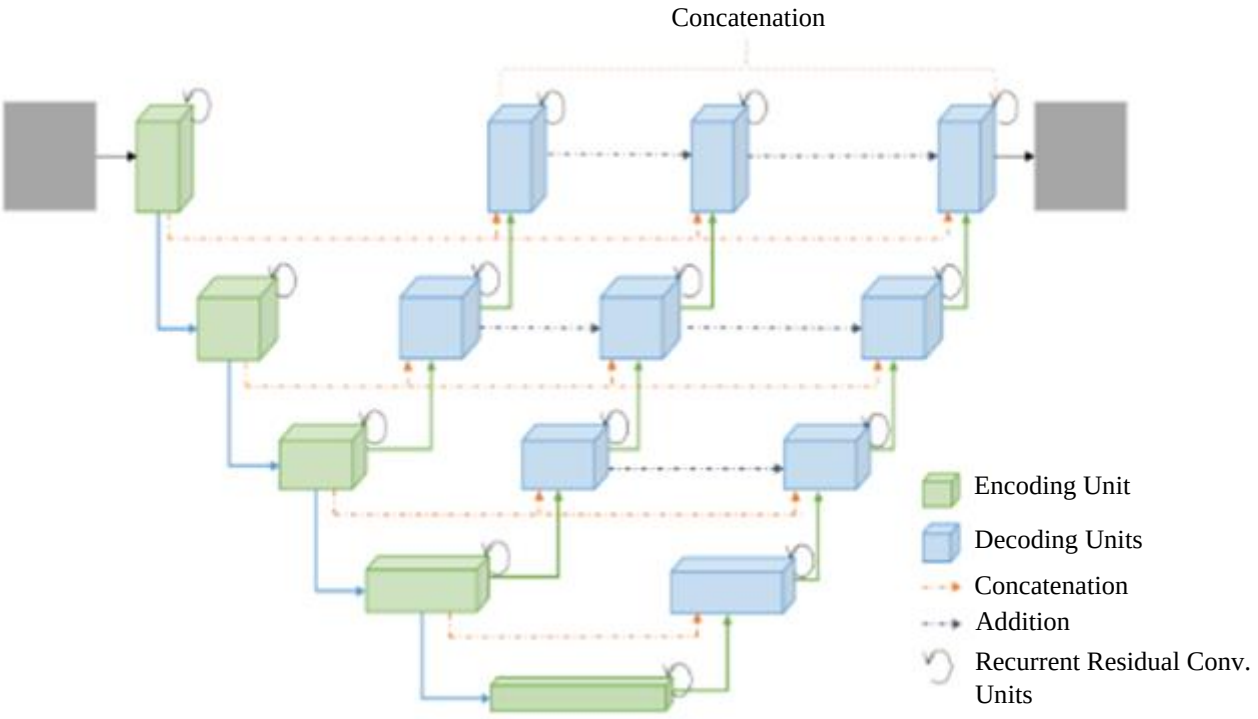

Fig. 3 The U-Net structure for implementing the feature classification based 7 class for the HAM10000 dataset

4.1. Design Approach for IWT-AWT Model

The segmenting feature is demonstrated with the IWT-AWT transform model improvising the different affected regions via improved Watershed and active watershed segments. The two features improved Watershed and active Watershed, are effectively characterized by the formulations of the discrete transform via an improved filtering approach with different transformation segments via projections. These projections are the points and distances from the skin-affected cell implicating the region of importance, namely ROI.

This feature from [11] has been utilized with a covariance matrix estimated with the critical features of entropy, kurtosis, mean, standard deviation and other parametric utilized to encapsulate the ROI values. The IWT is utilized to implicate the surrounding region with semantic segmentation, as mentioned below. The overall region segments will differ from the size of the lesion chosen with benign and melanoma.

Let X and Y be the overall random possibilities for which the transformation with Watershed is implemented with weights and matrix for $\varphi \in \mathscr{L}^2(\mathbb{R})$ which defines the square of Integrable function with Watershed transform as denoted by:

$$\varphi(x) = \int_0^{\infty} F(x) e^{-\frac{2\pi x}{N}} dx \quad (1)$$

Let X be the random variable for the $\varphi(x > X)$, $\varphi(x < X), \varphi(x == X)$ are the three possible scenarios for which the regions are estimated.

Let Y be the variable for each type of region to be estimated, as shown in the figure. Now Y_i defines the different boundaries estimation for each type of X_i determines the possible scenarios of greater, lesser, and equal to X. Since the image region with two-dimensionality are defined as

$$\varphi(x, y) = \int_0^{k} \int_k^{\infty} F(y) F(x) e^{-\frac{2\pi x}{N}} e^{-\frac{2\pi y}{N}} dxdy \quad (2)$$

While the finite region is defined as:

$$\varphi(x, y) = \sum_0^{k-1} \sum_k^N f(x) f(y) * z^{-\frac{nx}{k}} z^{\frac{-ny}{k}} \quad (3)$$

Let x_0 be the threshold point for the region to be estimated while y_0 the melanoma region is estimated as shown in the figure, while others are depicted with weight prediction algorithm as proposed with EC algorithms.

$$\varphi(x > x_0, y) = \sum_0^{k_0 - 1} \sum_{k=k_0}^N f(x > x_0) f(y) * z^{-\frac{nx_0}{k}} z^{\frac{-ny}{k}} \quad (4)$$

Similarly, for lesser conditions, we can observe the $x < x_0$,

$$\varphi(x < x_0, y) = \sum_0^n \sum_{k=k_0}^{k_0} f(x > x_0) f(y) * z^{-\frac{nx_0}{k}} z^{\frac{-ny}{k}} \quad (5)$$

4.1.1. IWT-Weight Prediction Algorithm

Input : m_i be the linear weight of the transformation IWT

Output : M be the output weight for transformation. Initiate the M with random initial weights varying from (0,1).

Iterate the loop for the size of image chosen

$m(0) \leftarrow \text{entropy(I)}$

$M \leftarrow m(0) * X(0) + m(1) * X(1) + m(2) * X(2) \ldots . m(a)X(a, b, c)$

Itieratetill$x < X \& x > X$

end.

4.1.2. AWT-IWT Algorithm

Input : I, be the input images for which regions are estimated in $\varphi \in \mathcal{L}^2(\mathbb{R})$.

Output : $\varphi(X, Y)$

Initiate the Images with an estimated threshold via the weight prediction algorithm as above.

Estimate the values of the weights from the Weight prediction algorithm.

iterate the loops with different weight values

$$\varphi\big(x == X(0)\big) \leftarrow kutosis(I) * e^{\text{entropy(I)}}$$

$$\varphi(x, y) \leftarrow \sum_0^{k-1} \sum_k^N f(x) f(y) * z^{-\frac{nX_0}{k}} z^{\frac{-ny}{k}}$$

$$\varphi(x > x_0, y) \leftarrow \sum_0^{k_0 - 1} \sum_{k=k_0}^N f(x > x_0) f(y) * z^{-\frac{nx_0}{k}} z^{\frac{-ny}{k}}$$

end.

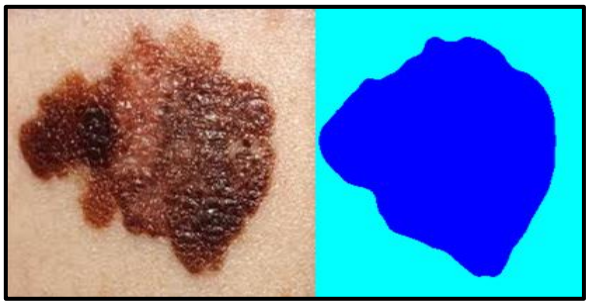

Fig. 4 The ROI calculated with the IWT algorithm as proposed

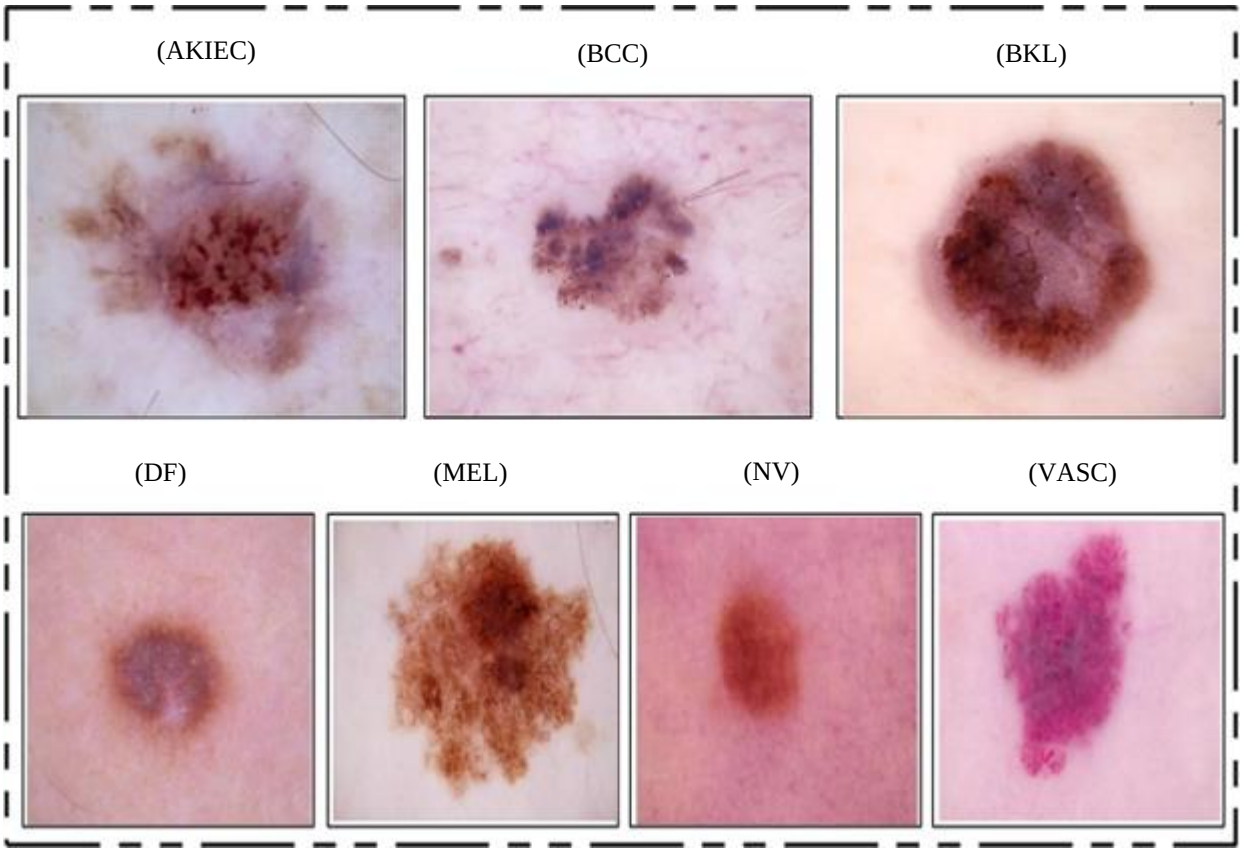

Fig. 5 The seven classes for skin cancer types

image_nar	patient_id	sex	age_apprc	anatom_si	diagnosis	benign_ma	target
ISIC_2637	IP_727996	male	45	head/neck	unknown	benign	0
ISIC_0015	IP_307518	female	45	upper extr	unknown	benign	0
ISIC_0052	IP_284207	female	50	lower extr	nevus	benign	0
ISIC_0068	IP_689042	female	45	head/neck	unknown	benign	0
ISIC_0074	IP_872331	female	55	upper extr	unknown	benign	0
ISIC_0074	IP_295048	female	40	lower extr	unknown	benign	0
ISIC_0074	IP_469828	male	25	lower extr	unknown	benign	0
ISIC_0075	IP_601720	female	35	torso	unknown	benign	0
ISIC_0075	IP_762288	male	30	torso	unknown	benign	0
ISIC_0076	IP_507553	female	50	lower extr	unknown	benign	0
ISIC_0076	IP_980260	male	55	upper extr	unknown	benign	0
ISIC_0076	IP_231816	male	75	upper extr	unknown	benign	0
ISIC_0076	IP_223534	female	55	torso	nevus	benign	0

Fig. 6 The ISIC dataset for classification feature using MATLAB

The above two algorithms inculcate the overall transformed feature for the semantic segmentation, as shown in the above figure representing the overall conditional changes. Other images on Nevus and Melanoma are utilized for classifying the different labels using Matlab, as shown in the results and discussion section.

4.2. Implementation

4.2.1. Pre-processing

The most significant feature acquisition stage for lesion segments to analyze for the specific learning algorithms depends on this stage. In this phase, our design on Nevus and Melanoma is utilized for each set of skin types and textures. The design's initial phase is utilized to remove unwanted features on the skin and its segmentation via a hybrid filter.

A concatenation of the Median and Threshold filter is implicated to form a segmented feature, as displayed in the results section.

The edge features are represented with K_x Threshold via 3x3 matrix as shown below:

$$K_x = \begin{matrix} 0 & -1 & 1 \\ -1 & 2 & 0 \\ -1 & -3 & -1 \end{matrix}$$

The proposed segmentation is represented with a combination of Gabor filter with gradients and directive gradients on the 3x3 matrix generated as mentioned above. The lesion segments are implicated with different colour spaces from labels to RGB, and RGB to label for each type of estimating the correct region is identified. Finally, we apply morphological operations to analyze the occurrence of the output image via gradient segments.

4.2.2. Classification

The classification mechanism is utilized with tabulation comparison on the dataset chosen ISIC, which comprises seven classes of cancer types and 6000 images to utilize the classification. The proposed IWT-AWT model is estimated with two classification features: Nevus and Melanoma. Since these two cancer types are more related to similar structural features hence challenging to classify them apart from categorical classification. Figure 5 depicts the seven classes of images utilized to classify the images' different features based on the IWT-AWT model. The classification methods represent the training and testing phase in the results and discussion section.

5. Results and Discussion

5.1. Dataset Acquisition

The overall design is implemented with two phases via images and dataset creation and the existing dataset chosen. Our design was improvised with Images from the ISIC dataset via the Kaggle website for Nevus and me, and features are estimated via entropy estimation as mentioned below figures via hybrid filter segmentation regions. This feature incorporates other feature estimates via IWT and AWT transformation on the image to enrapture the correct region of the image.

5.2. Filter Formulation and Algorithm

5.2.1. Hybrid Filter Algorithm

Input : X be the Input images

Output : Y be the output images

Iterate the different colour features on each type of image chosen

$Y \leftarrow \text{zeros (sizeofinput)}$

$\text{if } (x > k_a)$

$$Y \leftarrow \sum_{i=1}^{N} \max_{i<k} X_i * (k_{x_i})$$

else

$Y \leftarrow 0$

end

Pseudo Code

```
for  i=2:length ®
     if (r[I, 4]>20 && r{I, 4}<=35
          Rxl (I,2) = 1;
     else
          Rxl (I, 2) =0;
     end
end
```

For each feature class, we initiate the region based on age, location position, and diagnosis feature. We compare with filtered outputs on each class model and apply IWT and AWT models with different learning models.

We have also implemented this feature for four machine learning algorithms with a deep learning model on CNN. The overall classification accuracy and other performance features are represented in the table.

5.2.2. Segmented Regions

From the definition of the equation, 1-5 represents the different structural features of segmented regions and their analysis via the AWT algorithm. The feature region segmentation via IWT-AWT is represented via IWT for each set of images chosen from the directory.

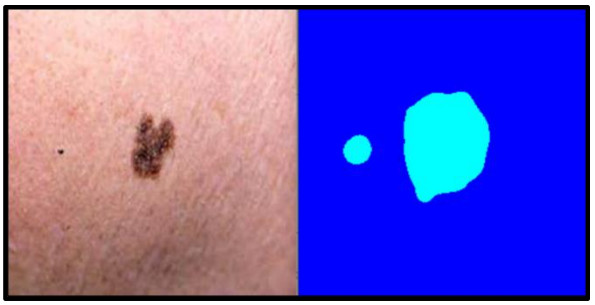

(a)

(b)

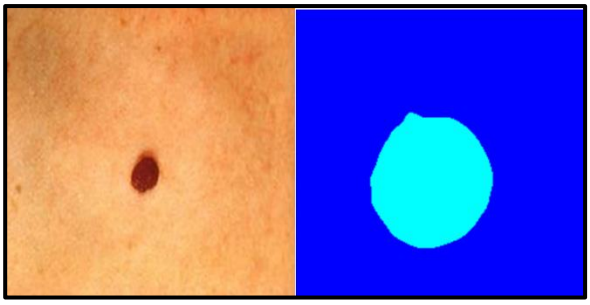

(c)

Fig. 7 The segmented and original feature using the IWT algorithm

Fig. 8 The AWT implementation on nevus images

The overall segmented region images are saved via write functionality to implicate the different segment classification features with Machine and deep learning algorithms.

5.3. Training and Testing

In this phase, we create 70 and 30 percent of training and testing samples for CNN and other learning algorithms as represented via dataset feature classification on ISIC images. In the CNN feature, our design with segmented images is analyzed and improvised with a region control model for each disease class chosen.

5.3.1. CNN Training Phase

In the training phase, we have implicated the different features of the segmentation models via IWT-AWT algorithms separately and conclusively for each image input from the directory inculcating the different principal components on the images chosen. This analysis generates a data table depending upon the features utilized with Watershed wavelet transforms. Finally, another set of images with 30 % is implemented for test features.

In this testing phase, all those 30 % of data are reutilized with the different functional features estimated via the IPA-AWT algorithm encapsulating the different mathematical values for each type of image. We create a threshold margin using AWT for labelling with different weights on the image chosen. Finally, these labelled weights would represent the class features and their classification based on the algorithms chosen. In our design, KNN, DT, Ensemble and stacking classifiers are implemented to classify Nevus and Melanoma images and ISIC dataset with feature filter classification as mentioned above.

5.3.2. Testing Phase

Table 3 depicts that CNN fails to outperform since only 30 (high-quality) images are chosen for the classification. In contrast, other algorithms have a consistent output for the images and dataset chosen. Different values are observed with an 8% improvement for the proposed algorithms with IWT-AWT with KNN, DT, Ensemble, and stacking classifiers.

In Figure 12, the overall design implementation of ABCD, SVM and KNN algorithms are plotted with an accuracy ranging from 66.9 to 83.6 as calculated based on the formulations of SVM and KNN algorithms.

The Conditions for sensitivity and specificity are observed by the formulation as mentioned:

$$Sensitivity = \frac{TruePositive}{(TruePos+False\ Neg)} \tag{6}$$

$$Specificity = \frac{TrueNeg}{(TrueNeg+FalsePos)} \tag{7}$$

The formulation from Eq. (6)-(7) represents the overall values observed in the 2X2 confusion matrix, which is implemented depending on the algorithm chosen. While the above formulations are utilized with structure as shown below matrix:

$$\text{CM} = \begin{matrix} True\ Positive & False\ Positive \\ Fasle\ Negative & True\ Negative \end{matrix} \tag{8}$$

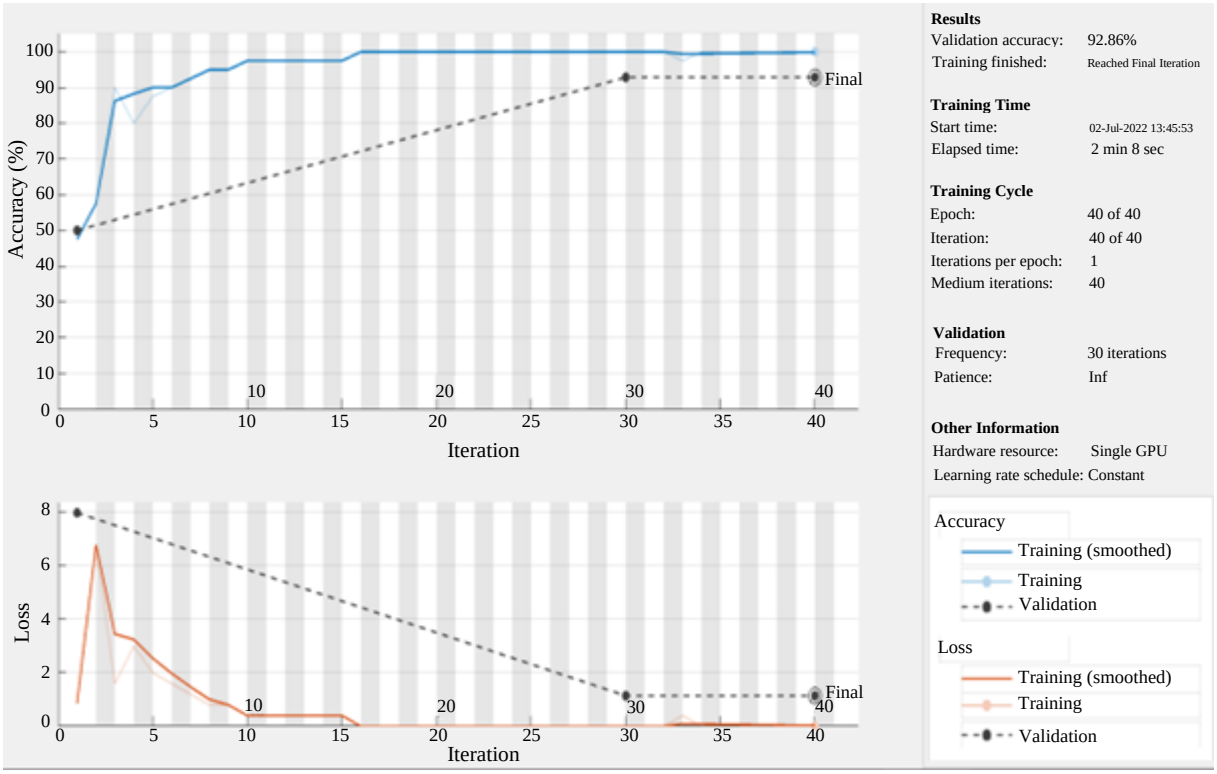

Fig. 9 The classification accuracy for the training phase in the proposed CNN

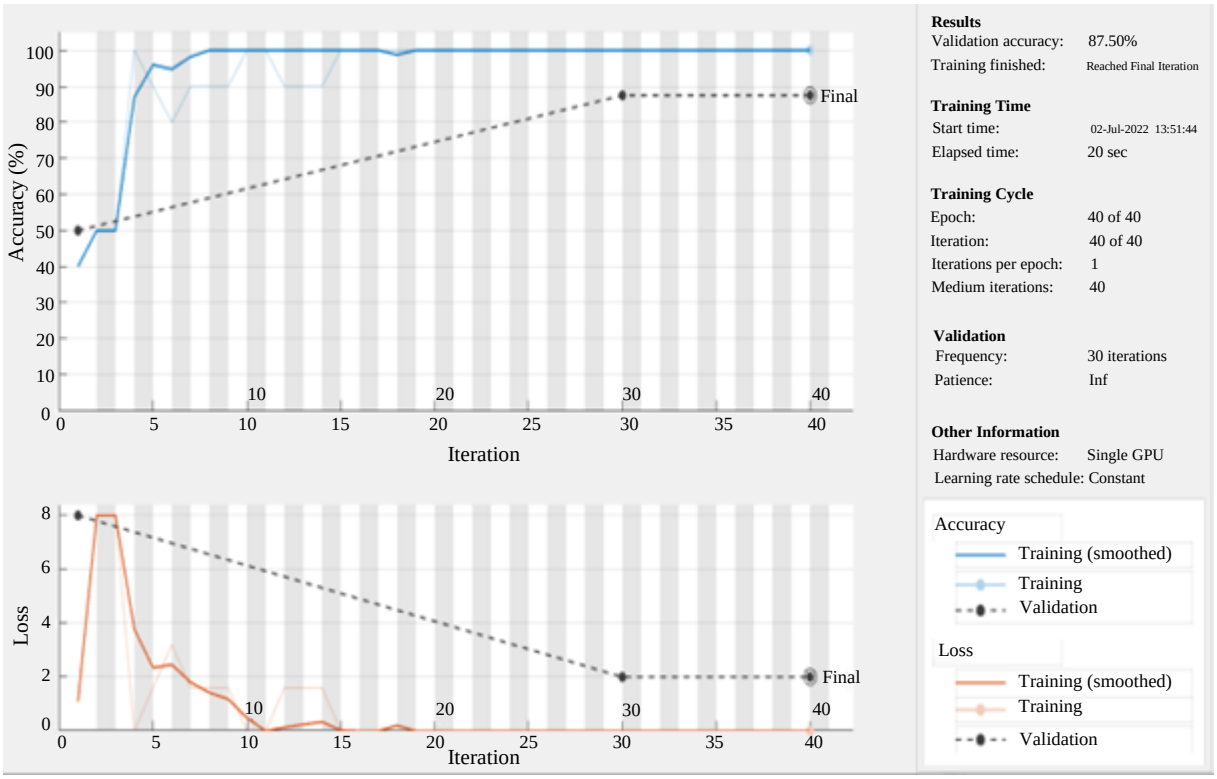

Fig. 10 The classification accuracy for the testing phase in the proposed CNN

Table 3. The different accuracies, sensitivity, and specificity values for the different algorithms implemented

S.No	Algorithm	Accuracy %	Sensitivity %	Specificity%
1	ABCD (existing) [6]	79.6	83.8	0
2	SVM (existing) [9]	83.6	86.93	23.7
3	KNN (existing) [12]	66.9	83.09	100
4	DT (IWT-AWT)	98.46	98.74	96.75
5	KNN (IWT-AWT)	98.46	94.75	91.84
6	Ensemble-BG (IWT-AWT)	98.46	86.75	96.53
7	Stacking Classifier (IWT-AWT)	98.68	94.92	97.45
8	CNN (IWT-AWT)	87.68	92.74	85.26
9	U-NET (SOA) [1]	93.64	95.23	97.23
10	CNN(SOA) [5]	95.42	94.21	96.14
11	SOA (GAN) [23]	99.18	99.53	99.47
12	Fuzzy GC-SCNN [9]	99.75	100	100

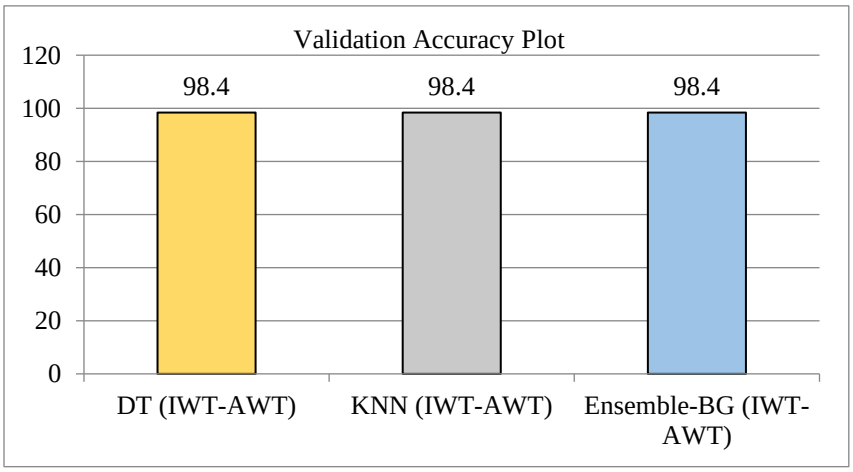

Fig. 11 The bar plot for accuracy for WKNN, DT and Ensemble algorithm with IWT-WT

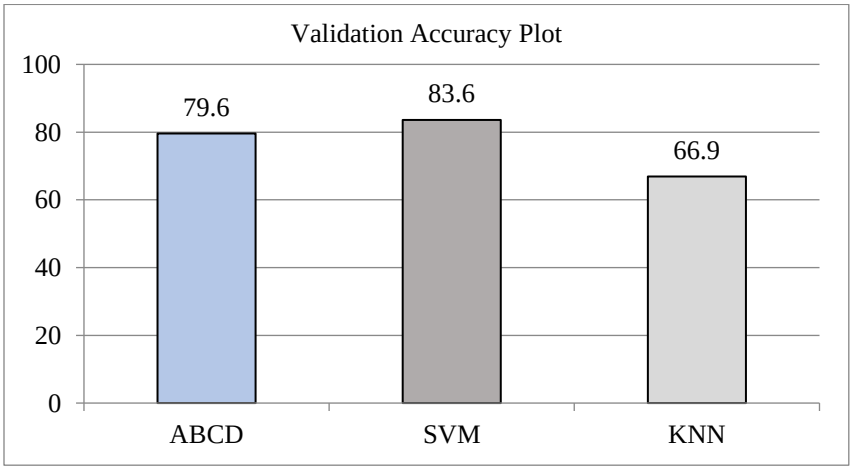

Fig. 12 The existing accuracies for algorithms ABCD, SVM and KNN

Hence, with this formulation for a confusion matrix, our design has obfuscated different weight features in the design model, which are activated by enabling weight values, the values with which all the algorithm functionality of identifying the skin cancer types. From the classification feature, specific weights are utilized to classify them as Nevus or Melanoma. With all the features utilized, MATLAB predefined functions with Confusion Matrix and accuracy score is calculated. The values are estimated with a formulation based on the confusion matrix identified using the confusion chart function. Since the labels are two Nevus and Melanoma, the results in 2x2 matrix as stated in Eq. (8). The observed values from the functionality formulations from Eq. (6-8) have represented in Matlab as formulated and represented in Fig. (12-15).

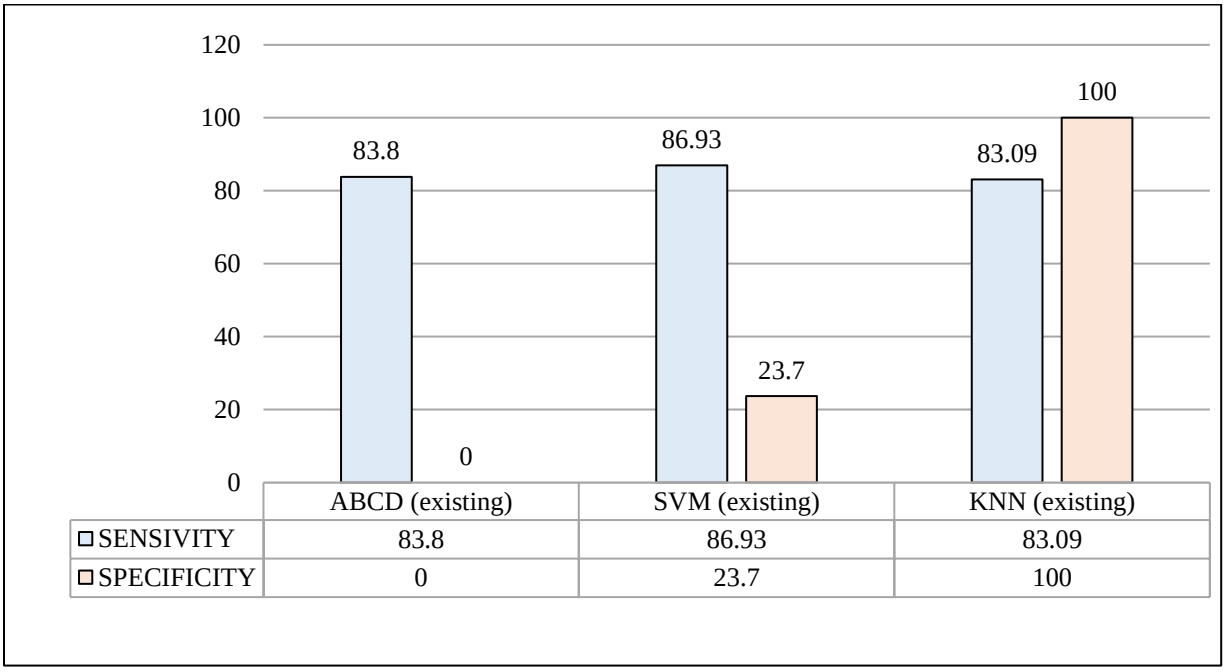

Fig. 13 The sensitivity and specificity with existing algorithms ABCD, SVM and KNN

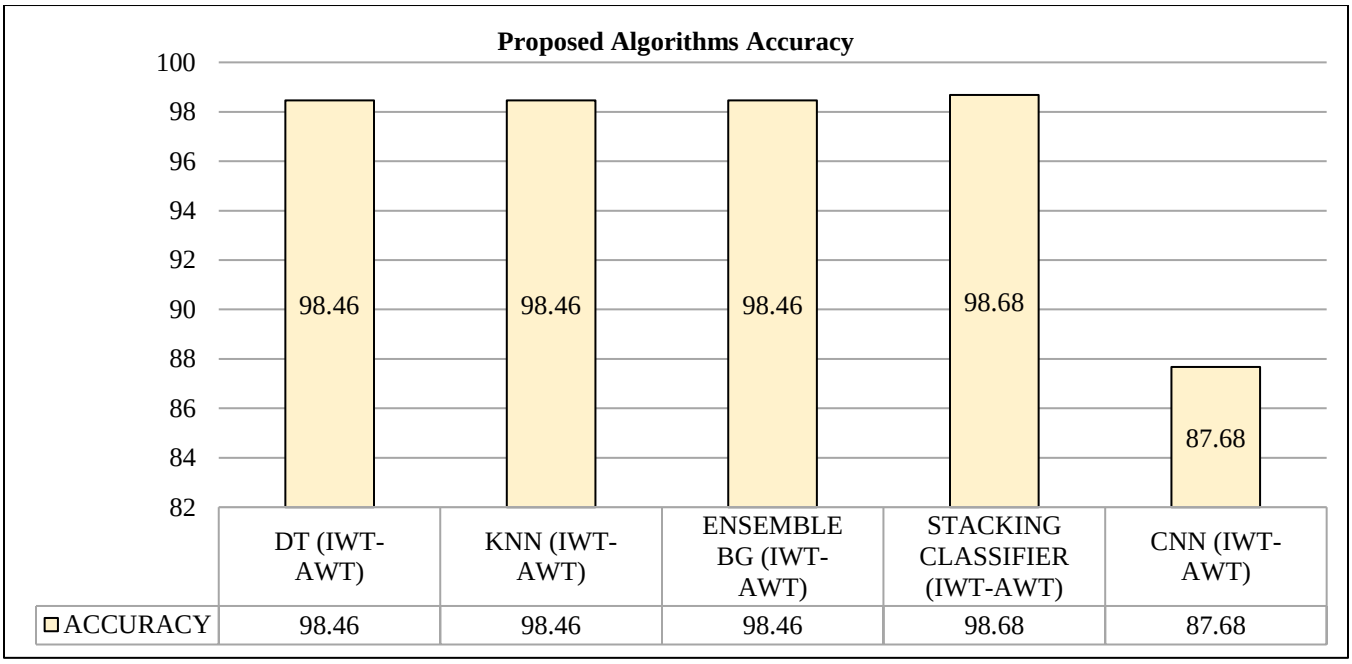

Fig. 14 The proposed accuracies for algorithms DT (IWT-AWT), KNN (IWT-AWT), CNN (IWT-AWT), ensemble-BG (IWT-AWT) and stacking (IWT-AWT)

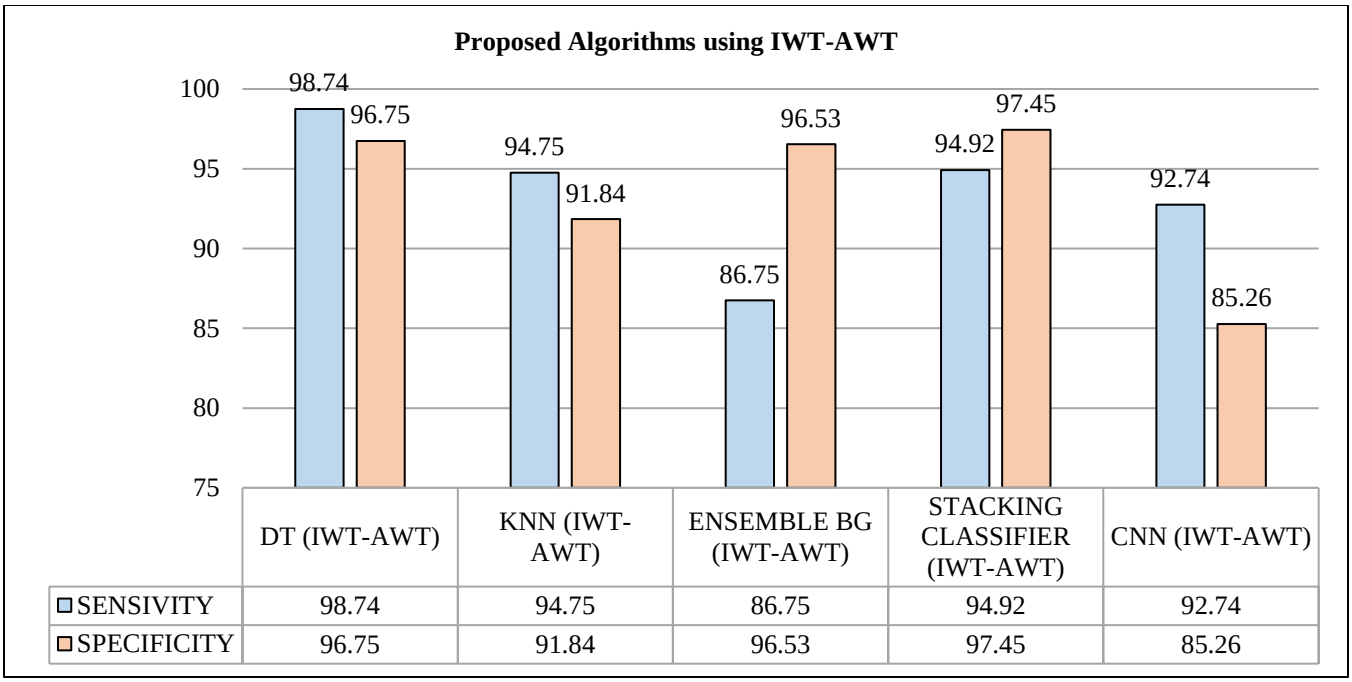

	DT (IWT-AWT)	KNN (IWT-AWT)	ENSEMBLE BG (IWT-AWT)	STACKING CLASSIFIER (IWT-AWT)	CNN (IWT-AWT)
SENSIVITY	98.74	94.75	86.75	94.92	92.74
SPECIFICITY	96.75	91.84	96.53	97.45	85.26

Fig. 15 The sensitivity and specificity with DT (IWT-AWT), KNN (IWT-AWT), CNN (IWT-AWT), ensemble-BG (IWT-AWT) and stacking (IWT-AWT)

6. Conclusion

In this paper, we have successfully compared our proposed work which outperforms most of the SOA architectures, including the references in [1, 5, 6, 9, 12, 23], indicating the best performance features for the models as proposed. Since the algorithm IWT-AWT improvises the customization of CNN, other algorithms have depicted far better results when compared to CNN, CNN (SOA), and other machine learning algorithms. At the same time, the only comparative results in [9] show that our proposed systems fail to attain the highest sensitivity and specificity. While the observed results with different other architectures are compared with tabulations from table-3 represents, our proposed design is far superior in accuracy and, sensitivity, specificity as mentioned in figures 12-15.

In order to realize such problems with the current design, we need to improvise the design features with Tensor-Flow architectures with the custom realization of Network Loss parametric in our proposed design. Improvements with design perspective and its implementation criteria for IWT-AWT in Python must be discussed with reference [9].

6.1. Scope

The proposed design with Tensor-Flow architectures is to be defined with custom loss and other performance metrics on the Confusion matrix, indicating the overall accuracy with F1- score, Recall, and Precision values verified with each type of the algorithms chosen for comparison.

Refernces

[1] Burcu Bılgıç, “Comparison of Breast Cancer and Skin Cancer Diagnoses using Deep Learning Method,” *2021 29th Signal Processing and Communications Applications Conference (SIU)*, Istanbul, Turkey, pp. 1-4, 2021. [CrossRef] [Google Scholar] [Publisher Link]

[2] Chee Jen Ngeh et al., “Deep Learning on Edge Device for Early Prescreening of Skin Cancers in Rural Communities,” *2020 IEEE Global Humanitarian Technology Conference (GHTC)*, Seattle, WA, USA, pp. 1-4, 2020. [CrossRef] [Google Scholar] [Publisher Link]

[3] Haseeb Younis, Muhammad Hamza Bhatti, and Muhammad Azeem, “Classification of Skin Cancer Dermoscopy Images using Transfer Learning,” *2019 15th International Conference on Emerging Technologies (ICET)*, Peshawar, Pakistan, pp. 1-4, 2019. [CrossRef] [Google Scholar] [Publisher Link]

[4] Agung W. Setiawan, “Effect of Color Enhancement on Early Detection of Skin Cancer using Convolutional Neural Network,” *2020 IEEE International Conference on Informatics, IoT, and Enabling Technologies (ICIoT)*, Doha, Qatar, pp. 100-103, 2020. [CrossRef] [Google Scholar] [Publisher Link]

[5] Paul Zhu, "Convolutional Neural Networks Based Study and Application for Multicategory Skin Cancer Detection," *2022 3rd International Conference on Electronic Communication and Artificial Intelligence (IWECAI)*, Zhuhai, China, pp. 558-561, 2022. [CrossRef] [Google Scholar] [Publisher Link]

[6] A. P. Abhiram, S. M. Anzar, and Alavikunhu Panthakkan, "Deep Skin Net: A Deep Learning Model for Skin Cancer Detection," *2022 5th International Conference on Signal Processing and Information Security (ICSPIS)*, Dubai, United Arab Emirates, pp. 97-102, 2022. [CrossRef] [Google Scholar] [Publisher Link]

[7] Prachya Bumrungkun, Kosin Chamnongthai, and Wisarn Patchoo, "Detection Skin Cancer using SVM and Snake Model," *2018 International Workshop on Advanced Image Technology (IWAIT)*, Chiang Mai, Thailand, pp. 1-4, 2018. [CrossRef] [Google Scholar] [Publisher Link]

[8] Khalid Zaman et al., "Analysis and Classification of Skin Cancer Images using Convolutional Neural Network Approach," *2020 4th International Symposium on Multidisciplinary Studies and Innovative Technologies (ISMSIT)*, Istanbul, Turkey, pp. 1-8, 2020. [CrossRef] [Google Scholar] [Publisher Link]

[9] Usharani Bhimavarapu, and Gopi Battineni, "Skin Lesion Analysis for Melanoma Detection using the Novel Deep Learning Model Fuzzy GC-SCNN," *Healthcare*, vol. 10, no. 5, pp. 1-14, 2022. [CrossRef] [Google Scholar] [Publisher Link]

[10] G. R. Meghana, Suresh Kumar Rudrahithlu, and K. C. Shilpa, "Detection of Brain Cancer using Machine Learning Techniques A Review," *SSRG International Journal of Computer Science and Engineering*, vol. 9, no. 9, pp. 12-18, 2022. [CrossRef] [Publisher Link]

[11] Jignyasa Sanghavi, "A Novel Approach for Detection of Skin Cancer using Back Propagation Neural Network Jignyasa Sanghavi," *Helix*, vol. 9, no. 6, pp. 5847-5851, 2019. [CrossRef] [Google Scholar] [Publisher Link]

[12] Swati Jayade, D. T. Ingole, and Manik D. Ingole, "Skin Cancer Detection using Gray Level Co-occurrence Matrix Feature Processing," *2020 5th International Conference on Devices, Circuits and Systems (ICDCS)*, Coimbatore, India, pp. 49-53, 2020. [CrossRef] [Google Scholar] [Publisher Link]

[13] Ayushi Kumar, Ari Kapelyan, and Avimanyou K. Vatsa, "Classification of Skin Phenotype: Melanoma Skin Cancer," *2021 IEEE Integrated STEM Education Conference (ISEC)*, Princeton, NJ, USA, pp. 247-247, 2021. [CrossRef] [Google Scholar] [Publisher Link]

[14] Jihe Zhu, Blagica Arsovska, and Kristina Kozovska, "Case Report - Fire-Needle Acupuncture Treatment in Skin Papillomas Located on the Neck," *SSRG International Journal of Medical Science*, vol. 6, no. 10, pp. 14-16, 2019. [CrossRef] [Google Scholar] [Publisher Link]

[15] Peddarapu Rama Krishna, and Pothuraju Rajarajeswari, "Early Detection of Melanoma Skin Cancer using Efficient Netb6," *2022 8th International Conference on Advanced Computing and Communication Systems (ICACCS)*, Coimbatore, India, pp. 01-05, 2022. [CrossRef] [Google Scholar] [Publisher Link]

[16] Ayasha Hossain Jui, Samia Sharnami, and Aminul Islam, "A CNN Based Approach to Classify Skin Cancers using Transfer Learning," *2022 25th International Conference on Computer and Information Technology (ICCIT)*, Cox's Bazar, Bangladesh, pp. 1063-1068, 2022. [CrossRef] [Google Scholar] [Publisher Link]

[17] Zhaojun Guo, Haobo Xu, and Tianhao Yao, "Multi-CNN Models with Pretraining for Binary Classification in Skin Cancer," *2022 3rd International Conference on Electronic Communication and Artificial Intelligence (IWECAI)*, Zhuhai, China, pp. 414-418, 2022. [CrossRef] [Google Scholar] [Publisher Link]

[18] Hari Antoni Musril et al., "Using k-NN Artificial Intelligence for Predictive Maintenance in Facility Management," *SSRG International Journal of Electrical and Electronics Engineering*, vol. 10, no. 6, pp. 1-8, 2023. [CrossRef] [Publisher Link]

[19] Lin Li, and Wonseok Seo, "Deep Learning and Transfer Learning for Skin Cancer Segmentation and Classification," *2021 IEEE 21st International Conference on Bioinformatics and Bioengineering (BIBE)*, Kragujevac, Serbia, pp. 1-5, 2021. [CrossRef] [Google Scholar] [Publisher Link]

[20] Zulaiha Parveen A, and T. Senthil Kumar, "The Deep Learning Methodology for Improved Breast Cancer Diagnosis in MRI," *International Journal of Computer and Organization Trends*, vol. 11, no. 3, pp. 11-14, 2021. [CrossRef] [Publisher Link]

[21] S. Likhitha, and Radhika Baskar, "Skin Cancer Classification using CNN in Comparison with Support Vector Machine for Better Accuracy," *2022 11th International Conference on System Modeling & Advancement in Research Trends (SMART)*, Moradabad, India, pp. 1298-1302, 2022. [CrossRef] [Google Scholar] [Publisher Link]

[22] Zehao Li, "A Skin Cancer Detection System Based on CNN with Hair Removal," *2023 IEEE 3rd International Conference on Power, Electronics and Computer Applications (ICPECA)*, Shenyang, China, pp. 1291-1294, 2023. [CrossRef] [Google Scholar] [Publisher Link]

[23] R. Gurumoorthy, and M. Kamarasan, "A Systematic Review on Deep Convolutional Neural Network-Based Breast Cancer Classification on Histopathological Images," *SSRG International Journal of Electronics and Communication Engineering*, vol. 10, no. 4, pp. 31-40, 2023. [CrossRef] [Publisher Link]

[24] Pooyan Sedigh, Rasoul Sadeghian, and Mehdi Tale Masouleh, "Generating Synthetic Medical Images by using GAN to Improve CNN Performance in Skin Cancer Classification," *2019 7th International Conference on Robotics and Mechatronics (ICRoM)*, Tehran, Iran, pp. 497-502, 2019. [CrossRef] [Google Scholar] [Publisher Link]

[25] Hari Kishan Kondaveeti, and Prabhat Edupuganti, "Skin Cancer Classification using Transfer Learning," *2020 IEEE International Conference on Advent Trends in Multidisciplinary Research and Innovation (ICATMRI)*, Buldhana, India, pp. 1-4, 2020. [CrossRef] [Google Scholar] [Publisher Link]

[26] S. Subha et al., "Detection and Differentiation of Skin Cancer from Rashes," *2020 International Conference on Electronics and Sustainable Communication Systems (ICESC)*, Coimbatore, India, pp. 389-393, 2020. [CrossRef] [Google Scholar] [Publisher Link]

[27] N. Nanthini et al., "Detection of Melanoma Skin Cancer using Deep Learning," *2022 3rd International Conference on Smart Electronics and Communication (ICOSEC)*, Trichy, India, pp. 1193-1197, 2022. [CrossRef] [Google Scholar] [Publisher Link]

[28] Melisa Uçkuner, and Hamza Erol, "A New Deep Learning Model for Skin Cancer Classification," *2021 6th International Conference on Computer Science and Engineering (UBMK)*, Ankara, Turkey, pp. 27-31, 2021. [CrossRef] [Google Scholar] [Publisher Link]